Molar volume of superfluid ^{3}He-^{4}He mixtures: The dependence of the Bardeen-Baym-Pines parameter on temperature, pressure, and ^{3}He concentration

Ken Hatakeyama,[1] Satoshi Noma,[2] Etsutaro Tanaka,[2] Serguei N. Burmistrov,[2,3] and Takeo Satoh[2,*]
[1]*Center for Low Temperature Science, Tohoku University, Sendai 980–8578, Japan*
[2]*Physics Department, Graduate School of Science, Tohoku University, Sendai 980–8578, Japan*
[3]*Kurchatov Institute, Moscow 123182, Russia*
(Received 12 April 2002; revised manuscript received 7 October 2002; published 14 March 2003)

We have developed a new method for determining the Bardeen-Baym-Pines (BBP) parameter of a superfluid ^{3}He-^{4}He mixture from the measurement of its molar volume within the wide ranges of temperature, pressure, and the ^{3}He concentration. The method and the results are described. The ranges of the present investigation are 0.4–660 mK in temperature, 0.3–10 kgf/cm^2 in pressure, and 0.07–0.39 in the ^{3}He concentration. The data obtained are fitted with a formula based on the phenomenological theory of dilute solutions of ^{3}He in superfluid ^{4}He. Our empirical formula can reproduce the experimental values of the BBP parameter within the accuracy of 1%. The argument on the absolute uncertainty is also given.

DOI: 10.1103/PhysRevB.67.094503 PACS number(s): 67.60.Fp, 67.80.Gb

I. INTRODUCTION

The molar volume V_m of a dilute solution of ^{3}He in ^{4}He (d-phase) is usually written in the form

$$V_m(T,P,x)=V_{40}(T,P)[1+\alpha(T,P,x)x], \tag{1}$$

where V_{40} is the molar volume of pure ^{4}He at the same temperature T and pressure P as a solution, and x is the molar concentration of ^{3}He. The number α is usually called the BBP parameter after Bardeen, Baym, and Pines (BBP),[1] who developed the theory of the dilute solution.

In our experimental investigation of the critical supersaturation in superfluid ^{3}He-^{4}He mixtures,[2] we are asked to determine the ^{3}He molar concentration x at various temperatures and pressures. We rewrite Eq. (1) as

$$x=\frac{1}{\alpha(T,P,x)}\left[\frac{V_m(T,P,x)}{V_{40}(T,P)}-1\right]. \tag{2}$$

This means that if the values of $\alpha(T,P,x)$ and $V_{40}(T,P)$ are known, then we can determine x from the measurement of $V_m(T,P,x)$.

Experimental efforts to determine the values of $\alpha(T,P,x)$ were done by various groups[3–6] just after the work of BBP. In our experiments of the critical supersaturation, the ranges are 0.4–645 mK in temperature, 1–8.5 kgf/cm^2 in pressure, and 0.07–0.39 in the ^{3}He molar concentration. (We use the unit of pressure kgf/cm^2 since this unit is already employed for the measurements in Ref. 2 which are closely related to the present study. The conversion to the SI unit is 1 kgf/cm^2 = 0.980665×10^5 Pa.) For such wide ranges, it is impossible to estimate the values of $\alpha(T,P,x)$ from the data published.[3–6] The ranges of parameters covered in Refs. 3–6 are tabulated in Table I. Note that all the experiments[3–6] were done by condensing a gas mixture, the ^{3}He concentration of which being known beforehand. Such way is not practical when one must handle a wide range of the ^{3}He concentration.

We have developed a completely different method to determine the BBP parameter $\alpha(T,P,x)$. In this report we present our method and show the results with it. The results are compared quantitatively with the calculated values based on the phenomenological theory along the analogous arguments given by Abraham *et al.*[5,7] Our empirical formula for $\alpha(T,P,x)$ can reproduce the experimental values within the accuracy of 1%.

II. EXPERIMENTAL

A. Principle of the method

The sample cell is schematically shown in Fig. 1. It contains a capacitor of the coaxial cylindrical shape for measuring the dielectric constant of mixtures, ϵ_m. We assume that the molar volume V_m is related to its dielectric constant by the Clausius-Mossotti relation

$$\frac{\epsilon_m-1}{\epsilon_m+2}=\frac{4\pi}{3}\frac{\chi}{V_m} \tag{3}$$

and that the molar polarizability χ is independent of density and temperature. Furthermore we assume that χ is same for ^{3}He and ^{4}He. We take the value from Kerr and Sherman[8] as

$$\chi=0.1232\ \text{cm}^3/\text{mol}\,. \tag{4}$$

TABLE I. The ranges of parameters covered in Refs. 3–6 for the investigation of the molar volume of ^{3}He-^{4}He mixtures.

Ref.	^{3}He concentration	Temperature[mK]	Pressure[atm]
3	0.06	1250–2200	0–20
4	0.02–0.15 (6 samples)	25–1200	0
5	0.055	38–525	0
6	0.064–0.10 (4 samples)	50–500	0–22.5

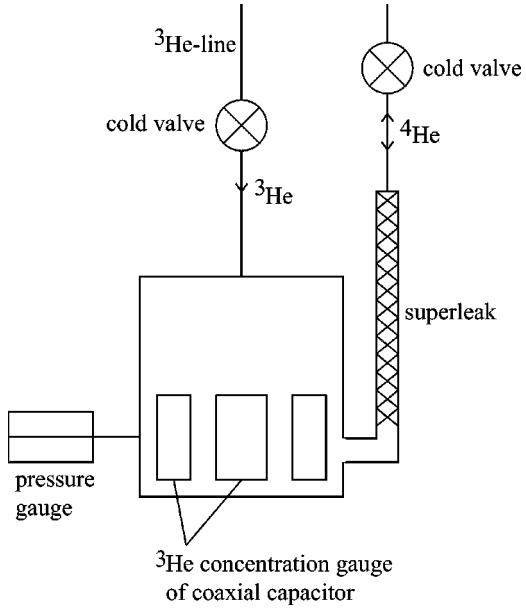

FIG. 1. Principal construction of the experimental cell.

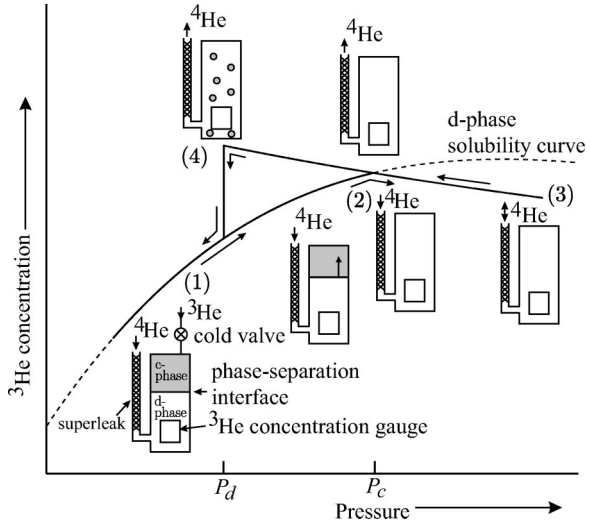

FIG. 2. Illustration of the method. The depressurization process (3)→(4) is used for the determination of the BBP parameter.

A cold valve[9] is equipped in the ^{3}He condensing line in order to keep constant the amount of ^{3}He in the cell during each series of experiments. Let us suppose that we have a single d-phase mixture in the sample cell of volume Ω at temperature T and pressure P, which consists of $\mathcal{N}_3$ moles of ^{3}He and $\mathcal{N}_4$ moles of ^{4}He. Then we have the relation

$$\Omega = (\mathcal{N}_3 + \mathcal{N}_4) V_m(T,P,x), \tag{5}$$

where the ^{3}He molar concentration is

$$x = \frac{\mathcal{N}_3}{\mathcal{N}_3 + \mathcal{N}_4} = \frac{n_3}{n_3 + n_4} \equiv \frac{n_3}{n}. \tag{6}$$

Here, n_3 and n_4 are the number density of ^{3}He and ^{4}He, respectively. With Eqs. (1), (5), and (6), the BBP parameter is expressed as

$$\alpha(T,P,x) = \frac{\Omega[V_m(T,P,x) - V_{40}(T,P)]}{\mathcal{N}_3 V_{40}(T,P) V_m(T,P,x)}. \tag{7}$$

This is the equation with which we determine the BBP parameter. The equation means that when the values of $V_{40}(T,P)$, Ω, and $\mathcal{N}_3$ are known, $\alpha(T,P,x)$ is obtained from the measurement of $V_m(T,P,x)$.

The sample cell has a superleak-line through which only the zero-entropy superfluid component of ^{4}He flows into the cell to pressurize the sample mixture, or out to depressurize it. The pressure is measured with a capacitance-type pressure gauge.[10] The cold valve in the ^{4}He-line is for the purpose of avoiding any pressure disturbance at the time of the transfer of liquid helium.

The method is illustrated in Fig. 2. First, pure ^{4}He is condensed into the cell through the superleak. Then, ^{3}He is condensed through the ^{3}He-line, during which ^{4}He flows out through the superleak. After obtaining an appropriate ratio of the d-phase and the ^{3}He-concentrated phase (c-phase), the cold valve in the ^{3}He-line is closed in order to keep the amount of ^{3}He in the cell, $\mathcal{N}_3$, constant. Then, we stabilize the temperature and start adding ^{4}He continuously into the cell through the superleak [(1) in Fig. 2]. The increase of the amount of ^{4}He in the cell, $\mathcal{N}_4$, causes a transformation of the c-phase into the d-phase due to the increase of the ^{3}He solubility with pressure[6] and the increase of the ratio $\mathcal{N}_4/\mathcal{N}_3$ in the cell. So the phase-separation interface moves up. The c-phase disappears at P_c [(2) in Fig. 2] and then the whole liquid enters into the unsaturated d-phase. We stop the pressurization in the unsaturated state far from the solubility curve [(3) in Fig. 2]. After obtaining the equilibrium state in the unsaturated region, we start the depressurization process. The process is continued until we observe a sudden demixing at P_d [(4) in Fig. 2]. During the depressurization process [(3)→(4) in Fig. 2], we have only a single d-phase. This depressurization process is used to determine $\alpha(T,P,x)$ with Eq. (7). In the present investigation, the sweep rate of pressure is always about 0.2 kgf/cm^2 h.

B. Molar volume of pure liquid ^{4}He

Although there have been various data published on the molar volume of pure liquid ^{4}He, $V_{40}(T,P)$,[6,11] those are not enough to obtain an empirical analytic expression for $V_{40}(T,P)$ which covers our experimental ranges of temperature and pressure. So, we determined $V_{40}(T,P)$ by ourselves and established a useful empirical formula which can give $V_{40}(T,P)$ within the accuracy of $\pm 5\times 10^{-4}$ cm^3/mol. The details can be found in Ref. 12.

C. Procedures to determine $\alpha(T,P,x)$

The experimental cell is the same as given in Ref. 2. In order to describe the present procedures clearly, the cell is reproduced in Fig. 3. It has two concentration gauges of capacitance type. They are separated by about 120 mm in order to check the homogeneity of the ^{3}He concentration. The lower one is called d-gauge as it is always wholly immersed in the d-phase. The other is placed at the top of the cell and

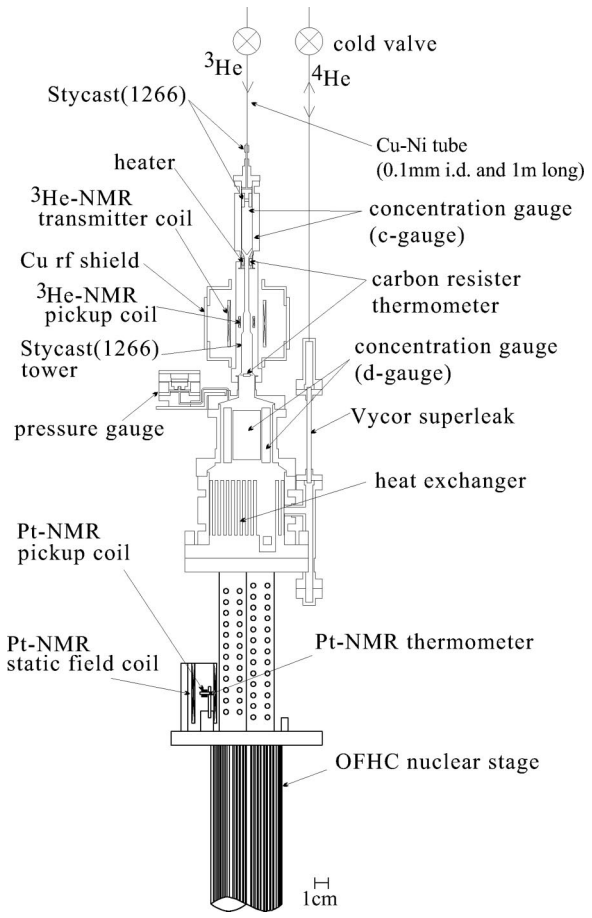

FIG. 3. Schematic diagram of the sample cell.

is called c-gauge because it is filled with the c-phase before starting the pressurization process. In the present investigation we use only the d-gauge. The c-gauge is used for the check of the homogeneity of the mixture and for the estimation of $\mathcal{N}_3$.

The effective volume of the cell is measured at the liquid nitrogen temperature and we take the value

$$\Omega = 77.3 \text{ cm}^3 \tag{8}$$

within the accuracy of 0.1%.

The details of the construction and the calibration procedure of the concentration gauge including the correction factor due to a possible deformation caused by the pressure are given in Ref. 12.

The procedures of determining $\alpha(T,P,x)$ are as follows.

(i) The amount of the ^{3}He condensed and confined in the cell is roughly estimated from the nuclear magnetic resonance (NMR) measurement of ^{3}He and by using the c-gauge. The value is denoted by $\mathcal{N}_{3,\mathrm{NC}}$. We move the position of the phase-separation interface through the NMR pick-up coil and the c-gauge by sweeping the pressure [see Figs. 2 and 3]. As the detailed numerical sizes of the various parts of the cell are known, the estimation of $\mathcal{N}_{3,\mathrm{NC}}$ is done fairly accurately.

(ii) Assuming $\mathcal{N}_3 = \mathcal{N}_{3,\mathrm{NC}}$ in Eq. (7), we obtain $\alpha(T,P,x)$ from the measured value of $V_m(T,P,x)$ with the d-gauge in the depressurization process (3)→(4) in Fig. 2. The BBP parameter thus obtained is denoted by $\alpha_{exp}(T,P;\mathcal{N}_{3,\mathrm{NC}})$. Note that the ^{3}He concentration x is a function of T and P as we are in the single d-phase region with a fixed amount of ^{3}He. The procedure is performed at various constant temperatures. From the data we make the plots of $\alpha_{exp}(T,P=\text{const.};\mathcal{N}_{3,\mathrm{NC}})$. All the plots are fitted with an appropriate polynomial

$$\alpha_{exp,fit}(T,P;\mathcal{N}_{3,\mathrm{NC}}) = \sum_{i=0}^{3} a_i(P;\mathcal{N}_{3,\mathrm{NC}}) T^{2i}, \tag{9}$$

where the coefficients on the right-hand side (rhs) of Eq. (9) are polynomials of the pressure determined by the method of least squares.

(iii) The amount of the c-phase which appears after the demixing [(4)→(1) in Fig. 2] is very small compared with the total amount of ^{3}He in the d-phase. So, we may use the determined $\alpha_{exp,fit}(T,P;\mathcal{N}_{3,\mathrm{NC}})$ even after the demixing. The calculated value of x with Eq. (2) in the two-phase region is the saturated concentration of ^{3}He in the d-phase, $x_{s,exp}(T,P)$.

We refer to the reliable data for the pressure dependence of the saturated ^{3}He concentration at 50 mK by Watson *et al.*,[6] $x_{s,\mathrm{W}}(0.05,P)$. Their data are plotted in Fig. 4 and fitted with a polynomial

$$x_{s,\mathrm{W}}(0.05,P) = \sum_{i=0}^{4} e_i P^i. \tag{10}$$

The coefficients e_i are given in Table II and the fitted curve is shown in Fig. 4. We compare our $x_{s,exp}(0.05,P)$ with $x_{s,\mathrm{W}}(0.05,P)$. If we do not have a good agreement between them, we slightly change the value of $\mathcal{N}_3$ from $\mathcal{N}_{3,\mathrm{NC}}$ and proceed with the same procedure described in (ii). We repeat until we have a good agreement between $x_{s,exp}(0.05,P)$ and $x_{s,\mathrm{W}}(0.05,P)$ within 0.0001 in the ^{3}He concentration. The finally determined value of $\mathcal{N}_3$ is denoted by "$\mathcal{N}_3$." We denote the corresponding BBP parameter by $\alpha_{exp}(T,P;\text{"}\mathcal{N}_3\text{"})$ and the fitting expression by $\alpha_{exp,fit}(T,P;\text{"}\mathcal{N}_3\text{"})$. In Fig. 5, we show the case of "$\mathcal{N}_3$"=0.207.

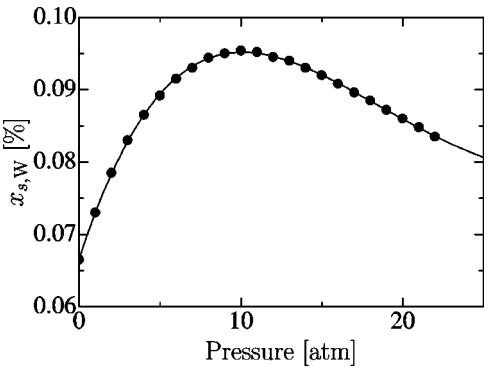

FIG. 4. The pressure dependence of the saturated ^{3}He concentration at 50 mK. The solid circles are the data by Watson *et al.* (Ref. 6). The solid curve is the fitting with Eq. (10).

TABLE II. The coefficients of the fitting polynomials of Eq. (10) and Eq. (13). The unit of pressure is chosen according to the original data (Refs. 6 and 13).

Equation	Coefficient	Value	Unit
Eq. (10)	e_0	6.66002676×10^{-2}	
	e_1	6.90439018×10^{-3}	$[\mathrm{atm}^{-1}]$
	e_2	-5.41249313×10^{-4}	$[\mathrm{atm}^{-2}]$
	e_3	1.50839054×10^{-5}	$[\mathrm{atm}^{-3}]$
	e_4	-1.43287300×10^{-7}	$[\mathrm{atm}^{-4}]$
Eq. (13)	f_0	9.91282623	$[\mathrm{K}^{-2}]$
	f_1	-9.45972330×10^{-1}	$[\mathrm{K}^{-2}\,\mathrm{bar}^{-1}]$
	f_2	1.14630208×10^{-1}	$[\mathrm{K}^{-2}\,\mathrm{bar}^{-2}]$
	f_3	-5.64035730×10^{-3}	$[\mathrm{K}^{-2}\,\mathrm{bar}^{-3}]$
	f_4	1.01525599×10^{-4}	$[\mathrm{K}^{-2}\,\mathrm{bar}^{-4}]$

(iv) The procedure analogous to (iii) can be employed at various temperatures if we have a reliable expression for $x_s(T,P)$. Generally, the saturated concentration may be expressed as

$$x_s(T,P)=x_s(0,P)[1+\beta(P)T^2] \tag{11}$$

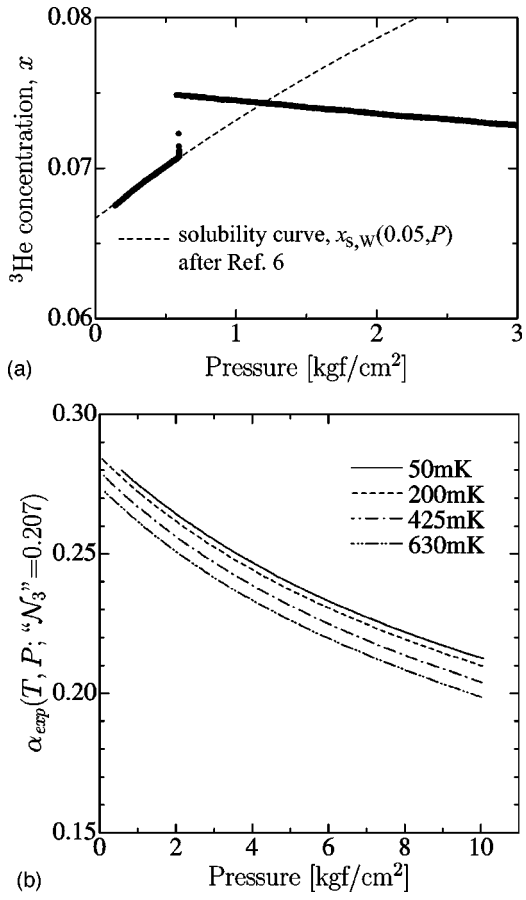

FIG. 5. Results for the series with "$\mathcal{N}_3$"$=0.207$ mol. (a) Comparison between $x_{s,exp}(0.05,P)$ and $x_{s,W}(0.05,P)$. (b) The determined $\alpha_{exp}(T,P;$"$\mathcal{N}_3$"$=0.207)$ is shown as a function of pressure at various constant temperatures.

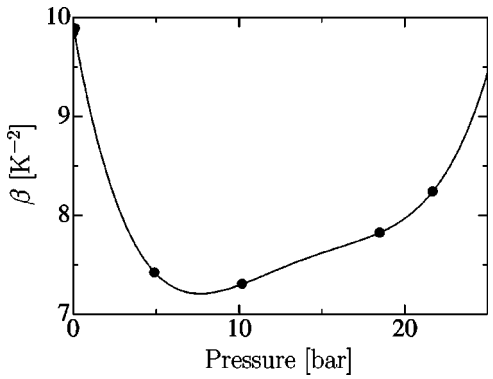

FIG. 6. The pressure dependence of the parameter $\beta(P)$ in Eq. (11). The solid circles are the data by Kurikawa (Ref. 13). The solid curve represents the fitting with Eq. (13).

in the region of the temperatures sufficiently low compared with the Fermi temperature $T_F(x_s)$. In order to fix the value of $x_s(T,P)$, we again use the value of $x_{s,W}(0.05,P)$. That is, from Eq. (11) we have

$$x_s(0,P)=\frac{x_{s,W}(0.05,P)}{1+\beta(P)\times(0.05)^2}. \tag{12}$$

For $\beta(P)$, we refer to the data by Kurikawa,[13] which are plotted in Fig. 6. We fit the data with a polynomial expression

$$\beta(P)=\sum_{i=0}^{4} f_i P^i. \tag{13}$$

The coefficients f_i are given in Table II and the fitted curve is shown in Fig. 6.

The examples of comparison between $x_{s,exp}(T,P)$ and $x_s(T,P)$ of Eq. (11) are shown in Fig. 7 at $T=12$ mK and $T=80$ mK for the case of "$\mathcal{N}_3$"$=0.273$. As can be seen, they are in a good agreement. This may mean the reliability

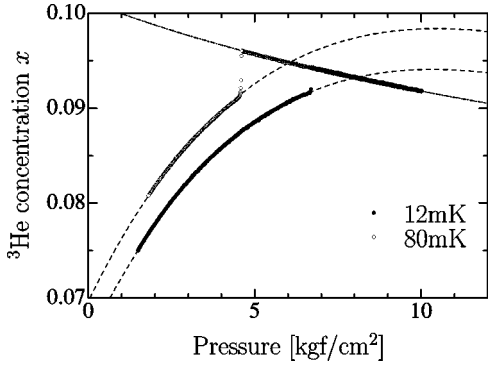

FIG. 7. Comparison between $x_{s,exp}(T,P)$ [solid circles: at 12 mK, open circles: at 80 mK] and the calculated $x_s(T,P)$ of Eq. (11) [dashed curves]. The dot-dash curve represents $x(T,P;$"$\mathcal{N}_3$"$=0.273)$ calculated with Eq. (2) by using $\alpha_{exp,fit}(T,P;$"$\mathcal{N}_3$"$=0.273)$. Note that the temperature dependence in the single d-phase region is very small. This can be understood as $\mathcal{N}_3$ is constant.

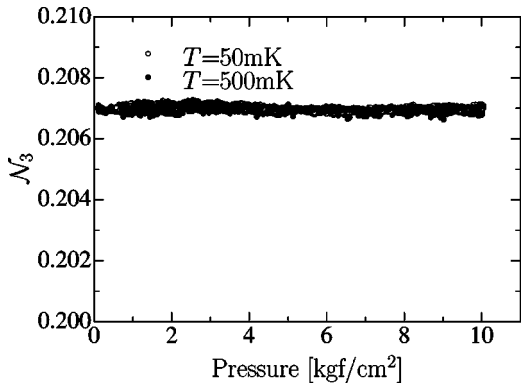

FIG. 8. The values of $\mathcal{N}_3$ obtained from Eq. (14) during the depressurization processes at $T=50$ mK and 500 mK in the series of "$\mathcal{N}_3$"=0.207.

of our values of "$\mathcal{N}_3$" and $\alpha_{exp}(T,P;\text{"}\mathcal{N}_3\text{"})$, and also the usefulness of the fitting formulas of Eqs. (10), (11), and (13).

In the phase-separated region, one must wait for a time to obtain an equilibrium state between the coexisting d- and c-phases. That time becomes longer remarkably with the increase of temperature.[2] In such high temperature regions, the comparison can be done only at $P=P_d$.

(v) The reliability of the values of "$\mathcal{N}_3$" and $\alpha_{exp,fit}(T,P;\text{"}\mathcal{N}_3\text{"})$ can be checked also by the following way.

With $\alpha_{exp,fit}$, we rewrite Eq. (7) as

$$\mathcal{N}_3=\frac{\Omega[V_m(T,P,x)-V_{40}(T,P)]}{\alpha_{exp,fit}(T,P;\text{"}\mathcal{N}_3\text{"})V_{40}(T,P)V_m(T,P,x)}. \quad (14)$$

Here, we consider $\mathcal{N}_3$ as unknown parameter. With Eq. (14) $\mathcal{N}_3$ is calculated from the measured value of $V_m(T,P,x)$ during the depressurization process [(3)→(4) in Fig. 2]. The calculated values of $\mathcal{N}_3$ should not depend on temperature and pressure.

The examples of such check are shown in Fig. 8. It is seen that $\mathcal{N}_3$ scatters around "$\mathcal{N}_3$" without any appreciable deviation. This check procedure can be performed regardless of the temperature region, because an equilibrium state is realized readily when the whole liquid is in the d-phase and the depressurization rate is as small as 0.2 kgf/cm^2 h.

A possible escape of ^{3}He through the cold valve and the superleak for a long time of experiments has proved to be nondetectable. The details can be found in Ref. 2 (2002).

We increase the amount of ^{3}He, $\mathcal{N}_3$, step by step and perform procedures (i)–(iii) at each step followed by procedures (iv) and (v). When $\mathcal{N}_3$ exceeds some amount, we always have a phase-separated state at 50 mK for any pressure. Then, procedure (iii) cannot be applied.

III. THEORETICAL

A. General expression for $\alpha(T,P,x)$

Let us consider a mixture at temperature T in the volume Ω with pressure P, which consists of $\mathcal{N}_3$ moles of ^{3}He and $\mathcal{N}_4$ moles of ^{4}He. The chemical potential per particle of the mixture μ is of the form

$$\mu(T,P,x)=x\mu_3(T,P,x)+(1-x)\mu_4(T,P,x), \quad (15)$$

where μ_3 and μ_4 are the chemical potential per particle of ^{3}He and ^{4}He in the mixture, respectively. The atomic volume of the mixture can be calculated by

$$v_m(T,P,x)=\left(\frac{\partial\mu}{\partial P}\right)_{T,x}. \quad (16)$$

With the Gibbs-Duhem relation, μ_4 is related to μ_3 by

$$\mu_4(T,P,x)=\mu_4(T,P,0)-\int_0^x\frac{x'}{1-x'}\frac{\partial\mu_3(T,P,x')}{\partial x'}dx'. \quad (17)$$

So, Eq. (15) is rewritten as

$$\begin{aligned}\mu(T,P,x)&=(1-x)\mu_4(T,P,0)+x\mu_3(T,P,x)\\&\quad-(1-x)\int_0^x\frac{x'}{1-x'}\frac{\partial\mu_3(T,P,x')}{\partial x'}dx' \quad (18)\\&=(1-x)\mu_4(T,P,0)+(1\\&\quad-x)\int_0^x\frac{\mu_3(T,P,x')}{(1-x')^2}dx'. \quad (19)\end{aligned}$$

The energy of a ^{3}He quasiparticle excitation of small momentum p in the mixture may be expressed as

$$\epsilon_p=\epsilon_0(P)+\frac{p^2}{2m^*(P)}+\epsilon_{int}(P,x,p). \quad (20)$$

The first two terms are the energy in the dilute limit and the effective mass m^* depends only on the pressure. The last term is the contribution from the ^{3}He-^{3}He interaction. Therefore, the ^{3}He chemical potential in the mixture can be represented in the form[5]

$$\mu_3(T,P,x)=\epsilon_0(P)+\mu_F(T,P,x)+x\epsilon_1(T,P,x), \quad (21)$$

where μ_F is the chemical potential of a free Fermi gas of effective mass $m^*(P)$. Substituting Eq. (21) into Eq. (18) or (19), we obtain

$$\begin{aligned}\mu(T,P,x)&=(1-x)\mu_4(T,P,0)+x\epsilon_0(P)+(1-x)\\&\quad\times\int_0^x\frac{x'}{(1-x')^2}\epsilon_1(T,P,x')dx'+x\mu_F(T,P,x)\\&\quad-(1-x)\int_0^x\frac{x'}{1-x'}\frac{\partial\mu_F(T,P,x')}{\partial x'}dx'. \quad (22)\end{aligned}$$

The equation of state of a free Fermi gas is obtained from the following two equations:[14]

$$n_3\lambda^3=f_{3/2}(z), \quad (23)$$

$$\frac{\lambda^3 P_F}{k_B T} = f_{5/2}(z), \tag{24}$$

where P_F is usually called the Fermi pressure, λ is the thermal de Broglie's wavelength,

$$\lambda = \left(\frac{2\pi\hbar^2}{m^* k_B T} \right)^{1/2}, \tag{25}$$

and

$$f_{5/2}(z) = \frac{4}{\sqrt{\pi}} \int_0^\infty dx x^2 \ln\{1 + z \exp(-x^2)\},$$

$$f_{3/2}(z) = z \frac{\partial}{\partial z} f_{5/2}(z). \tag{26}$$

The chemical potential μ_F is related to z by

$$\mu_F = k_B T \ln z. \tag{27}$$

The Fermi temperature is given as

$$T_F = \frac{\hbar^2 (3\pi^2 n_3)^{2/3}}{2 m^* k_B}. \tag{28}$$

By partially differentiating Eq. (24), we have

$$\left[\frac{\partial}{\partial P} \left(\frac{\lambda^3 P_F}{k_B T} \right) \right]_{T,x} = \frac{d f_{5/2}(z)}{dz} \left(\frac{\partial z}{\partial P} \right)_{T,x} \tag{29}$$

and

$$\left[\frac{\partial}{\partial x} \left(\frac{\lambda^3 P_F}{k_B T} \right) \right]_{T,P} = \frac{d f_{5/2}(z)}{dz} \left(\frac{\partial z}{\partial x} \right)_{T,P}. \tag{30}$$

In the same way with Eq. (27), we have

$$\left(\frac{\partial \mu_F}{\partial P} \right)_{T,x} = \frac{k_B T}{z} \left(\frac{\partial z}{\partial P} \right)_{T,x} \tag{31}$$

and

$$\left(\frac{\partial \mu_F}{\partial x} \right)_{T,P} = \frac{k_B T}{z} \left(\frac{\partial z}{\partial x} \right)_{T,P}. \tag{32}$$

With Eqs. (29) and (31), we obtain

$$\left(\frac{\partial \mu_F}{\partial P} \right)_{T,x} = \frac{1}{n_3} \left(\frac{\partial P_F}{\partial P} \right)_{T,x} + \frac{P_F}{n_3 \lambda^3} \left(\frac{\partial \lambda^3}{\partial P} \right)_{T,x}, \tag{33}$$

where we use Eqs. (23) and (26). With Eq. (25), Eq. (33) is transformed into

$$\left(\frac{\partial \mu_F}{\partial P} \right)_{T,x} = \frac{1}{n_3} \left(\frac{\partial P_F}{\partial P} \right)_{T,x} - \frac{3}{2} \frac{P_F}{n_3} \frac{1}{m^*} \frac{dm^*}{dP}. \tag{34}$$

With Eqs. (30) and (32), we obtain

$$\left(\frac{\partial \mu_F}{\partial x} \right)_{T,P} = \frac{1}{n_3} \left(\frac{\partial P_F}{\partial x} \right)_{T,P} = \frac{1}{nx} \left(\frac{\partial P_F}{\partial x} \right)_{T,P}, \tag{35}$$

where we use Eqs. (23), (26), and (6).

Substituting Eq. (35) into the last term on the rhs of Eq. (22), we obtain

$$\mu(T,P,x) = (1-x)\mu_4(T,P,0) + x\epsilon_0(P) + (1-x) \times \int_0^x \frac{x'}{(1-x')^2} \epsilon_1(T,P,x') dx' + x\mu_F(T,P,x) - \frac{x}{n_3} P_F(T,P,x) + \frac{x(1-x)}{n_3} \int_0^x \frac{P_F(T,P,x')}{(1-x')^2} dx'. \tag{36}$$

Employing Eq. (36) for Eq. (16), we have the expression for $v_m(T,P,x)$. Then with Eq. (1), the BBP parameter is expressed as

$$\alpha(T,P,x) = \alpha_1(T,P) + \alpha_2(T,P,x) + \alpha_3(T,P,x) + \alpha_4(T,P,x) + \alpha_5(T,P,x), \tag{37}$$

where

$$\alpha_1(T,P) = n_{40}(T,P) \frac{d\epsilon_0}{dP} - 1, \tag{38}$$

$$\alpha_2(T,P,x) = n_{40}(T,P) \frac{P_F}{n_3} \left\{ \frac{1}{n_3} \left(\frac{\partial n_3}{\partial P} \right)_{T,x} - \frac{3}{2} \frac{1}{m^*} \frac{dm^*}{dP} \right\}, \tag{39}$$

$$\alpha_3(T,P,x) = n_{40}(T,P) \frac{1-x}{x} \int_0^x \frac{x'}{(1-x')^2} \times \left[\frac{\partial \epsilon_1(T,P,x')}{\partial P} \right]_{T,x'} dx', \tag{40}$$

$$\alpha_4(T,P,x) = n_{40}(T,P) \frac{1-x}{n_3} \int_0^x \frac{1}{(1-x')^2} \times \left[\frac{\partial P_F(T,P,x')}{\partial P} \right]_{T,x'} dx', \tag{41}$$

$$\alpha_5(T,P,x) = -n_{40}(T,P) \frac{1-x}{n_3^2} \left(\frac{\partial n_3}{\partial P} \right)_{T,x} \times \int_0^x \frac{P_F(T,P,x')}{(1-x')^2} dx'. \tag{42}$$

Here we use Eq. (34) and

$$\left(\frac{\partial \mu_4(T,P,0)}{\partial P} \right)_T = v_{40}(T,P) = \frac{1}{n_{40}(T,P)} \tag{43}$$

is the atomic volume of pure liquid ^{4}He.

In the next section, we give further discussions on α_2, α_3, α_4, and α_5 and fix the approximate expression of $\alpha(T,P,x)$ for the present purpose to construct our empirical formula.

B. Basic idea for the approximate formula

Let us start with $\alpha_2(T,P,x)$. As is seen from Eq. (39), it is necessary to know the pressure dependence of m^* for the numerical estimation of $\alpha_2(T,P,x)$. The effective mass of ^{3}He in the dilute limit results from the motion of a ^{3}He atom in superfluid ^{4}He. This has a correspondence in the classical fluid mechanics, that is, the effective mass consists of the ^{3}He bare mass m_3 and the induced mass. Pandharipande and Itoh[15] made a microscopic calculation and gave the expression

$$\frac{m^*}{m_3}=\left[1-b\frac{n_{40}(0,P)}{n_{40}(0,0)}\right]^{-1}, \tag{44}$$

where the parameter b is determined to fit the experimental value of m^* at $P=0$. From the data published,[16] we take the value as the best fitting

$$b=0.56. \tag{45}$$

With the help of Eq. (44) α_2 can be expressed as a sum of terms

$$\alpha_2(T,P,x)\simeq\alpha_{20}(T,P,x)+\Delta\alpha_2(T,P,x), \tag{46}$$

where

$$\alpha_{20}=\frac{P_F}{n_3}\left\{\left[\frac{\partial n_{40}(T,P)}{\partial P}\right]_T - \frac{3}{2}\frac{n_{40}(T,P)}{m^*}\frac{dm^*}{dn_{40}(0,P)}\frac{dn_{40}(0,P)}{dP}\right\}, \tag{47}$$

$$\Delta\alpha_2(T,P,x)=-n_{40}(T,P)\frac{P_F}{n_3}\left[\frac{\partial\alpha_1(T,P)}{\partial P}\right]_T x. \tag{48}$$

The sense of such representation is that $\Delta\alpha_2(x)$ compared with $\alpha_{20}(x)$ is one order of the magnitude smaller in x, i.e., $\Delta\alpha_2\sim x\alpha_{20}$. In its turn, eliminating the parameter z from the exact Eqs. (23) and (24), using $n_3=$"$\mathcal{N}_3$"N_A/Ω, our empirical formula of $V_{40}(T,P)$,[12] and the expression for m^* of Eq. (44), the calculation of α_{20} can be performed as accurately as one wants.

Treating the last terms α_4 and α_5, one can see from Eqs. (41) and (42) that their order of magnitude in x does not exceed that of $\Delta\alpha_2$. For $T\ll T_F$, we estimate

$$\alpha_4+\alpha_5\simeq\frac{1}{10}\left(\frac{\partial n_{40}}{\partial P}\right)_T k_B T_F x=\frac{1}{10}\frac{P_F}{n_3}\left(\frac{\partial n_{40}}{\partial P}\right)_T x. \tag{49}$$

This could be compared with $\Delta\alpha_2$. However, the numerical estimation shows that $\Delta\alpha_2$ is about three times larger than a sum $\alpha_4+\alpha_5$. For the other limit of $T\gg T_F$, a ratio enhances more in favor of $\Delta\alpha_2$. The leading terms in α_4 and α_5, both proportional to x, cancel each other. Therefore, on the whole, we can neglect $\alpha_4+\alpha_5$ compared with $\Delta\alpha_2$.

The contribution to the ^{3}He chemical potential from the interaction at $T=0$ is of the form[7]

$$x\epsilon_1(0,P,x)=6nx\int_0^1 dy(1-y)y^2[2V(0)-V(2p_F y)], \tag{50}$$

where the second term comes from the exchange scattering and p_F is the Fermi momentum,

$$p_F=(3\pi^2 n_3)^{1/3}=(3\pi^2 n)^{1/3}x^{1/3}. \tag{51}$$

The quantity $V(q)$ is called the effective interaction between the ^{3}He atoms and the long wavelength limit for very dilute mixtures is given with our present notation as[1,7]

$$V(0)=-\alpha_1^2(0,P)\frac{m_4 s_{40}^2}{n_{40}}, \tag{52}$$

where m_4 is the ^{4}He bare mass and s_{40} is the sound velocity in liquid ^{4}He. Several empirical formulas for $V(q)$ were suggested in Refs. 1 and 17 based on the various experimental data[18] up to $x=0.05$. The suggested $V(q)$ shows the change of sign around $2p_F$ for the $x=0.023$ solution. So, we may expect that the contribution of the second term is much smaller than that of the first term in Eq. (50) for the mixtures of high concentrations studied here. To some extent, this can be justified by the final good fitting of the experimental results. Thus we assume that the second term can be neglected. Then, within the lowest approximation in x we have from Eq. (40)

$$\alpha_3(0,P,x)\simeq n_{40}(0,P)\left[\frac{\partial\epsilon_1(0,P,x\to 0)}{\partial P}\right]\frac{x}{2} \tag{53}$$

$$=-\frac{1}{2}n_{40}(0,P)m_4\left[\frac{\partial s_{40}^2(0,P)\alpha_1^2(0,P)}{\partial P}\right]x. \tag{54}$$

The next step in our speculation is an assumption that α_3 for a finite temperature conserves its functional dependence on the parameters concerned and thus is given by the temperature-dependent α_1 and s_{40} as

$$\alpha_3(T,P,x)\simeq-\frac{1}{2}n_{40}(T,P)m_4\left[\frac{\partial s_{40}^2(T,P)\alpha_1^2(T,P)}{\partial P}\right]x \tag{55}$$

$$=-\frac{1}{2}n_{40}(T,P)\left(\frac{\partial n_{40}}{\partial P}\right)^{-1} \times\alpha_1^2(T,P)\left[\frac{2}{\alpha_1}\frac{\partial\alpha_1}{\partial P}-\left(\frac{\partial n_{40}}{\partial P}\right)^{-1}\frac{\partial^2 n_{40}}{\partial P^2}\right]x, \tag{56}$$

where we use the relation

TABLE III. The list of our experiments tabulated alphabetically in the order of the amount of ^{3}He confined in the sample cell "$\mathcal{N}_3$." The columns of Temperature, Pressure, and ^{3}He concentration are the experimental ranges investigated.

Series	"$\mathcal{N}_3$" [mol]	Temperature [mK]	Pressure [kgf/cm^2]	^{3}He concentration
A	0.207	1–630	0.65–10	0.07–0.08
B	0.220	1–100	0.61–5	0.07–0.08
C	0.273	0.4–200	0.26–10	0.09–0.10
D	0.299	130–220	0.75–10	0.10–0.11
E	0.373	220–310	0.45–10	0.12–0.14
F	0.457	310–370	0.95–10	0.15–0.16
G	0.502	340–400	1.19–10	0.17–0.18
H	0.557	400–445	1.07–10	0.19–0.20
I	1.004	580–660	1.50–10	0.35–0.39

$$m_4 s_{40}^2 = \left(\frac{\partial n_{40}}{\partial P} \right)^{-1}. \tag{57}$$

Consequently, the approximate formula used for the present study is given as

$$\alpha(T,P,x) = \alpha_1(T,P) + \alpha_{20}(T,P,x) + \Delta\alpha_2(T,P,x) + \alpha_3(T,P,x) \tag{58}$$

with Eqs. (38), (47), (48), and (56). The formula generalizes the analogous one[5,7] derived in the limiting case of small concentration and is thus insufficient for a wide concentration range.

In the next section, we discuss our experimental results with Eq. (58) and try to fix the expressions of α_1 and $\Delta\alpha_2 + \alpha_3$ as the functions of T, P, and x. Note that α_{20}, the ideal Fermi gas contribution, can be treated exactly. So, there is no sense from the physical point of view to use a simple Taylor series in contrast to the other terms for which the theoretical description is not so transparent because of the ^{3}He-^{4}He and ^{3}He-^{3}He interactions.

IV. RESULTS AND DISCUSSIONS

We have performed nine series of experiments. In each succession, the amount of the ^{3}He confined in the sample cell, "$\mathcal{N}_3$," is kept constant as mentioned in Sec. II. The series are listed alphabetically from A to I in Table III with various experimental situations. Note that for series A, B, and C all the procedures described in Sec. II C are employed while for the series from D to I the procedure (iii) cannot be applied.

In the following, we first construct the empirical formula of the BBP parameter $\alpha_{emp,\mathrm{A}}$ with the data of a series A and Eq. (58). Then, applying $\alpha_{emp,\mathrm{A}}$ to the series from B to I, in which the ^{3}He concentration becomes higher and higher, we have to correct $\alpha_{emp,\mathrm{A}}$ by augmenting the term proportional to x^2.

A. Series A

The data of a series A are already shown in Fig. 5(b) where the values of α_{exp} determined in the depressurization processes at various constant temperatures are plotted as a function of pressure. From the data we obtain the plots of α_{exp} as a function of temperature at various constant pressures. Examples of such plots are given in Fig. 9.

As is noted in the preceding section, the numerical calculation of α_{20} can be done accurately. Our present calculation is within the accuracy of 0.1%. Examples of the results are shown in Fig. 10. As can be seen, the magnitude of α_{20} is of the order of a few hundredths. So, the calculation within 0.1% accuracy is sufficient for the present purpose to establish the empirical formula within the accuracy of 1%.

In order to estimate $\Delta\alpha_2$ and α_3, it is necessary to know $\alpha_1(T,P)$. The direct calculation with Eq. (38) is impossible as we have no data of $d\epsilon_0/dP$. We choose the method of successive approximation. That is, at first α_1 is estimated with

$$\alpha_1(T,P) = \alpha_{exp,fit}(T,P;0.207) - (\alpha_{20} + \Delta\alpha_2 + \alpha_3)_{\text{“}\mathcal{N}_3\text{”}=0.207}, \tag{59}$$

wherein the second term of the rhs $\alpha_{exp,fit}$ is used for α_1 in the formulas of $\Delta\alpha_2$ and α_3. Then, by employing thus ob-

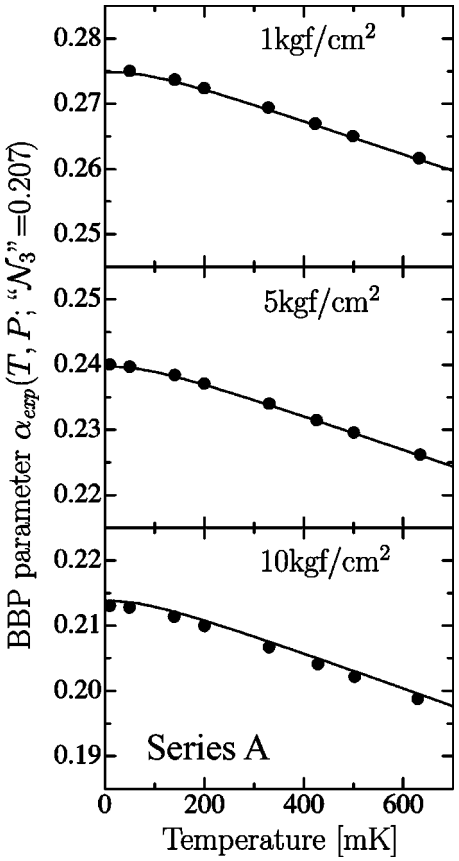

FIG. 9. $\alpha_{exp}(T,P;\text{“}\mathcal{N}_3\text{”}=0.207)$ is plotted as a function of temperature at various constant pressures. The solid curves are the calculated $\alpha_{emp,\mathrm{A}}$ of Eq. (68).

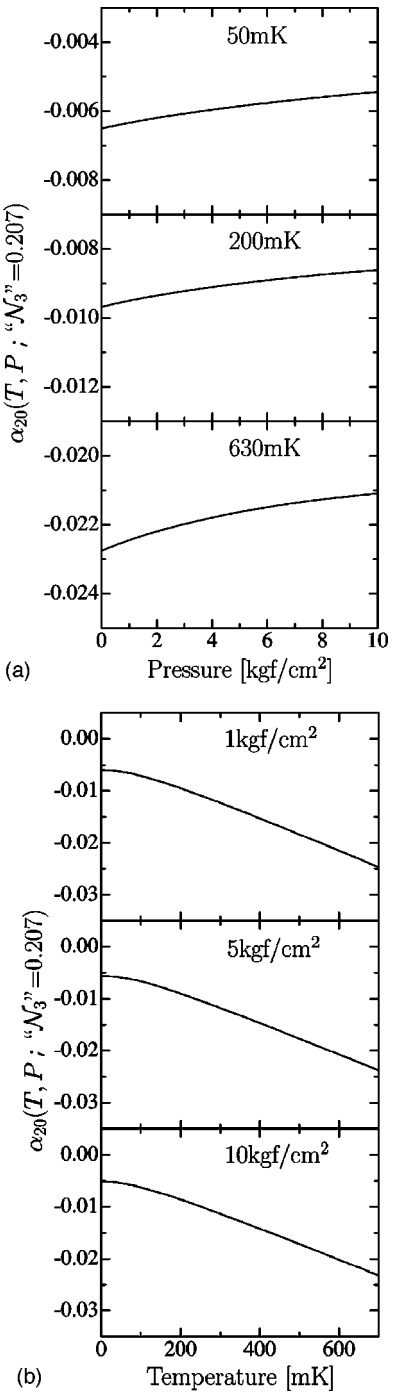

FIG. 10. Calculated α_{20} of Eq. (47) for the series of "$\mathcal{N}_3$"=0.207. (a) α_{20} is plotted as a function of pressure at various constant temperatures. (b) α_{20} is plotted as a function of temperature at various constant pressures.

tained α_1 for the calculation of $\Delta\alpha_2$ and α_3, we reestimate α_1 with Eq. (59). We repeat the procedure until we have a good convergence of α_1.

The finally determined $\alpha_1(T,P)$ is found to be fitted very well by the following polynomial of T and P:

$$\alpha_1(T,P)=A_{10}(P)+A_{11}(P)T, \tag{60}$$

where

TABLE IV. The coefficients of our empirical formulas of Eq. (61), Eq. (67), and Eq. (71).

Equation	Coefficient	Value	Unit
Eq. (61)	$A_{10,0}$	2.88069661×10^{-1}	
	$A_{10,1}$	-1.22906885×10^{-2}	$[(\text{kgf/cm}^2)^{-1}]$
	$A_{10,2}$	8.96636618×10^{-4}	$[(\text{kgf/cm}^2)^{-2}]$
	$A_{10,3}$	-5.56080168×10^{-5}	$[(\text{kgf/cm}^2)^{-3}]$
	$A_{10,4}$	1.98453350×10^{-6}	$[(\text{kgf/cm}^2)^{-4}]$
	$A_{11,0}$	3.44136785×10^{-3}	$[\text{K}^{-1}]$
	$A_{11,1}$	-3.64987971×10^{-4}	$[\text{K}^{-1}\cdot(\text{kgf/cm}^2)^{-1}]$
	$A_{11,2}$	9.05825884×10^{-5}	$[\text{K}^{-1}\cdot(\text{kgf/cm}^2)^{-2}]$
	$A_{11,3}$	-6.90965963×10^{-6}	$[\text{K}^{-1}\cdot(\text{kgf/cm}^2)^{-3}]$
Eq. (67)	$A_{31,00}$	7.37459686×10^{-2}	
	$A_{31,01}$	-1.31948465×10^{-2}	$[(\text{kgf/cm}^2)^{-1}]$
	$A_{31,02}$	1.15781554×10^{-3}	$[(\text{kgf/cm}^2)^{-2}]$
	$A_{31,03}$	-6.00790576×10^{-5}	$[(\text{kgf/cm}^2)^{-3}]$
	$A_{31,20}$	3.45606250×10^{-2}	$[\text{K}^{-2}]$
	$A_{31,21}$	-3.94265287×10^{-3}	$[\text{K}^{-2}\cdot(\text{kgf/cm}^2)^{-1}]$
	$A_{31,22}$	1.77228908×10^{-4}	$[\text{K}^{-2}\cdot(\text{kgf/cm}^2)^{-2}]$
Eq. (71)	$A_{32,00}$	-5.83958128×10^{-2}	
	$A_{32,01}$	3.22314921×10^{-3}	$[(\text{kgf/cm}^2)^{-1}]$
	$A_{32,02}$	2.67308396×10^{-4}	$[(\text{kgf/cm}^2)^{-2}]$
	$A_{32,10}$	6.41936151×10^{-2}	$[\text{K}^{-1}]$
	$A_{32,11}$	-4.13744209×10^{-3}	$[\text{K}^{-1}\cdot(\text{kgf/cm}^2)^{-1}]$
	$A_{32,12}$	3.24197589×10^{-4}	$[\text{K}^{-1}\cdot(\text{kgf/cm}^2)^{-2}]$

$$A_{10}(P)=\sum_{i=0}^{4}A_{10,i}P^i,$$

$$A_{11}(P)=\sum_{i=0}^{3}A_{11,i}P^i. \tag{61}$$

The coefficients of the polynomials of Eq. (61) are given in Table IV.

In Fig. 11, we show the plot of $\alpha_1(0,P)$. Note that $\alpha_1(0,0)$ is just $\alpha(0,0,x\rightarrow0)\equiv\alpha_0$. From Eqs. (60) and (61) we obtain

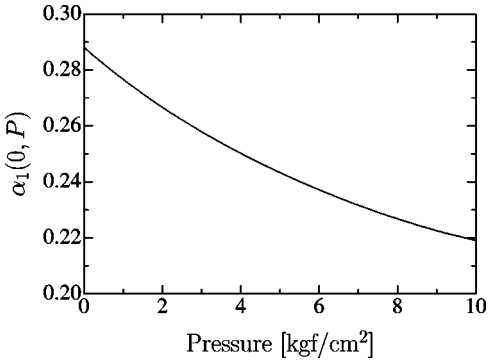

FIG. 11. $\alpha_1(0,P)$ calculated with Eq. (60) is shown as a function of pressure.

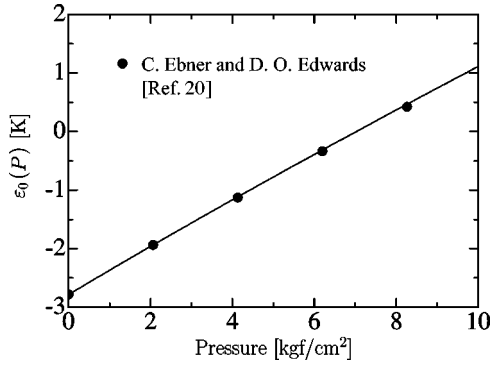

FIG. 12. The binding energy of a ^{3}He atom in pure ^{4}He, $\epsilon_0(P)$ [see Eq. (64)]. Here we use the value $\epsilon_0(0)=-2.785$ K from Ref. 19.

$$\alpha_0=0.288. \tag{62}$$

This value is in good agreement with the data published,

$$\alpha_0=0.284\pm0.005^4,$$

$$\alpha_0=0.286\pm0.001^5. \tag{63}$$

The pressure dependence of the BBP parameter was first studied in Refs. 3 and 6 in which the data extrapolated to the limit of $T=0$ K are given. However, either the limit of $x\rightarrow0$ was not considered at all or the concentration dependence was neglected within their experimental range.[6] The latter can be justified only in the low pressure range of $P=0$ (see Sec. IV C and Figs. 16[1], [2]). As far as we know, the present result of Eqs. (60) and (61) is the first case of empirical expression fitting the experimental pressure dependence of the BBP parameter in the limit of $T=0$ K and $x\rightarrow0$.

As can be seen from Table IV, the value of the second term on the rhs of Eq. (60) is very small compared with the first term. That is, $\alpha_1(T,P)$ is almost independent of temperature. We can calculate $\epsilon_0(P)$ with Eq. (38),

$$\epsilon_0(P)=\epsilon_0(0)+\int_0^P v_{40}(0,P')[\alpha_1(0,P')+1]dP'. \tag{64}$$

Taking the value of $\epsilon_0(0)=-2.785$ K from Ref. 19, we obtain $\epsilon_0(P)$ as shown in Fig. 12. In the figure, the quantity $\epsilon_0(P)$ calculated in Ref. 20 is also plotted for comparison. Although in Fig. 11 we did not show the magnitude of the BBP parameter used in Ref. 20, we recognize a systematic difference between our $\alpha_1(0,P)$ and the BBP parameter after Ref. 20. The difference increases with the growth of pressure, in particular, $\sim2\%$ at $P=2$ kgf/cm^2 and $\sim5\%$ at $P=8$ kgf/cm^2. As can be seen from Eq. (64) and Fig. 12, however, such small disagreement in the BBP parameter does not result in any appreciable difference for the magnitude of $\epsilon_0(P)$.

Since our aim is to establish an empirical formula as simple as possible, we combine $\Delta\alpha_2$ and α_3 and then try to fit it as

$$\tilde{\alpha}_3\equiv\Delta\alpha_2+\alpha_3=A_{31}(T,P)x. \tag{65}$$

From the finally determined $\Delta\alpha_2$ and α_3, it is found that $A_{31}(T,P)$ is fitted well by the polynomial of T and P,

$$A_{31}(T,P)=A_{31,0}(P)+A_{31,2}(P)T^2, \tag{66}$$

where

$$A_{31,0}(P)=\sum_{i=0}^{3}A_{31,0i}P^i,$$

$$A_{31,2}(P)=\sum_{i=0}^{2}A_{31,2i}P^i. \tag{67}$$

The coefficients of the polynomials of Eq. (67) are given in Table IV.

The empirical formula of the BBP parameter obtained with the data of series A can be summarized as

$$\alpha_{emp,\mathrm{A}}(T,P,x)=[A_{10}(P)+A_{11}(P)T]+\alpha_{20}(T,P,x)+[A_{31,0}(P)+A_{31,2}(P)T^2]x. \tag{68}$$

In Fig. 9, the solid curve in each figure represents the BBP parameter calculated with Eq. (68). As can be seen, the fitting is satisfactory as it should be.

B. Series B–I

The experimental data obtained for the series from B to I are shown in Fig. 13 where $\alpha_{exp}(T,P;\text{“}\mathcal{N}_3\text{”})$ is plotted as a function of pressure at various constant temperatures. In Fig. 14, the data are shown as a function of temperature at various constant pressures.

For each series, we calculate $\alpha_{emp,\mathrm{A}}$. The results are shown in Fig. 14 as dashed curves. It is seen that $\alpha_{emp,\mathrm{A}}$ deviates slightly from α_{exp} as “$\mathcal{N}_3$” increases. We suppose that the deviation arises from the increase of x with the increase of “$\mathcal{N}_3$.” So, we correct $\alpha_{emp,\mathrm{A}}$ by taking into account the contribution proportional to x^2. That is, we try to fit α_{exp} with

$$\alpha_{emp}(T,P,x)=\alpha_{emp,\mathrm{A}}(T,P,x)+A_{32}(T,P)x^2. \tag{69}$$

The polynomial $A_{32}(T,P)$ is determined to obtain the best fitting with the whole $\alpha_{exp}(T,P;\text{“}\mathcal{N}_3\text{”})$ by assuming the polynomial as simple as possible. The result is

$$A_{32}(T,P)=A_{32,0}(P)+A_{32,1}(P)T, \tag{70}$$

where

$$A_{32,0}(P)=\sum_{i=0}^{2}A_{32,0i}P^i,$$

$$A_{32,1}(P)=\sum_{i=0}^{2}A_{32,1i}P^i. \tag{71}$$

The coefficients of the polynominals of Eq. (71) are given in Table IV. The fittings are shown in Fig. 14 as solid curves.

This determination is done not only by obtaining the best fitting but also by employing procedure (v) in Sec. II C. That is, we calculate

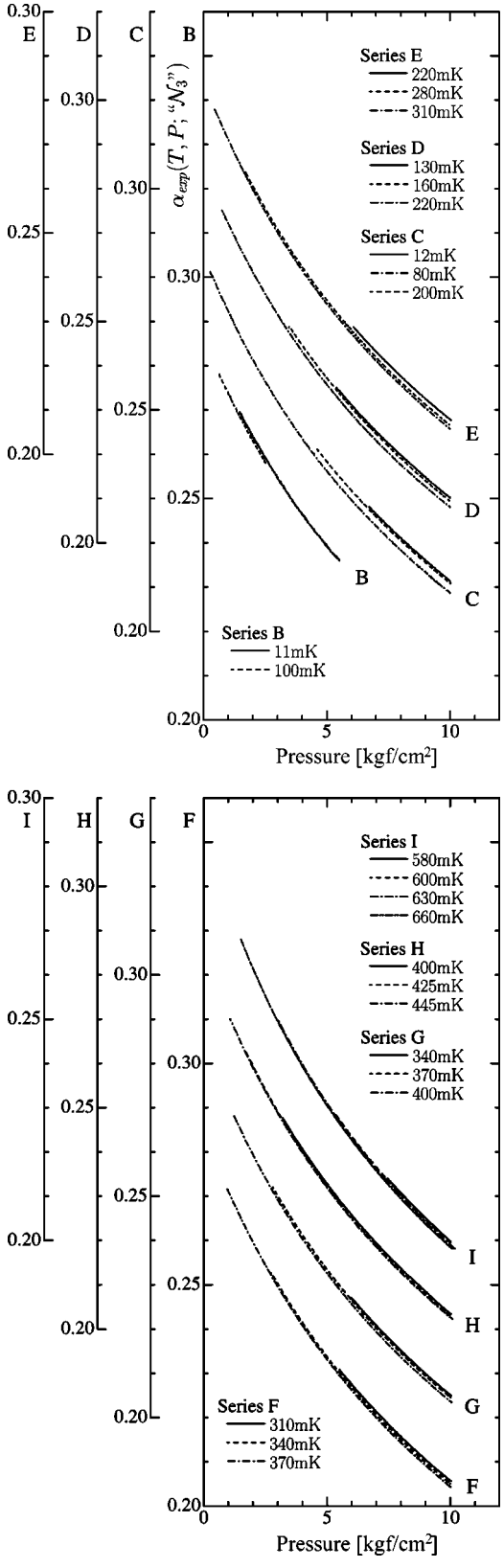

FIG. 13. Experimentally determined BBP parameter $\alpha_{exp}(T,P;\text{“}\mathcal{N}_3\text{”})$ is plotted as a function of pressure at various constant temperatures. The data are for series from B to I as described in Table III.

$$\mathcal{N}_3=\frac{\Omega[V_m(T,P,x)-V_{40}(T,P)]}{\alpha_{emp}(T,P;\text{“}\mathcal{N}_3\text{”})V_{40}(T,P)V_m(T,P,x)} \tag{72}$$

for all the series of experiments, The results are shown in Fig. 15. As can be seen, for each series the calculated values of $\mathcal{N}_3$ scatter around “$\mathcal{N}_3$” and they are almost independent of temperature and pressure, as it should be, within 1% of each “$\mathcal{N}_3$.”

Comparing Figs. 8 and 15 for “$\mathcal{N}_3$”=0.207, we notice that $\alpha_{emp,\mathrm{A}}$ is better than α_{emp} in the high pressure region above about 8 kgf/cm^2. In order to improve this point, we think that we should determine $\alpha_{emp,\mathrm{A}}$ by considering the x^2 term from the very beginning. However, from our present requirement to reproduce the BBP parameter within the accuracy of 1%, our formula α_{emp} is satisfactory.

Therefore, we may conclude that the empirical formula $\alpha_{emp}(T,P,x)$ of Eq. (69) reproduces our $\alpha_{exp}(T,P;\text{“}\mathcal{N}_3\text{”})$ satisfactorily, i.e., within the accuracy of 1%.

C. Concentration dependence of the BBP parameter

As can be seen from the formulas and figures presented so far, the pressure dependence of $\alpha_{emp}(T,P,x)$ arises mainly from that of $\alpha_1(T,P)$, and the temperature dependence is principally due to that of $\alpha_{20}(T,P,x)$. In this section, we examine the concentration dependence of $\alpha_{emp}(T,P,x)$. This seems interesting because our $\alpha_{emp}(T,P,x)$ is shown to be satisfactory at least up to $x\sim 0.4$, the highest concentration presently studied and, in addition, there has been no systematic study of the ^{3}He concentration dependence of the BBP parameter as a whole.

The examples of the results in the limit $T\rightarrow 0$ are shown in Figs. 16[1] and [2] for $P=0$ and 10 kgf/cm^2, respectively. In the figures, we also show the corresponding α_{20} and $\tilde{\alpha}_3 \equiv A_{31}x+A_{32}x^2$ as a function of x to recognize the competition between them. For $P=0$ kgf/cm^2, it is seen that the BBP parameter is very insensitive to the concentration in a wide range of concentration. Such behavior is consistent with the data published.[4,21] On the other hand, for $P=10$ kgf/cm^2, the BBP parameter shows a clear concentration dependence. Thus one recognizes that the concentration dependence varies considerably with pressure.

As the saturated ^{3}He concentration at $T=0$ is rather small, it may be interesting to see the behavior at a higher temperature. The concentration dependence at $T=0.69$ K under the saturated vapor pressure is reported in Ref. 4. The comparison between the data[4] and the calculation with Eq. (69) is shown in Fig. 16[3]. We note the difference of 1%–2.5%, depending on the concentration. Such noticeable discrepancy is not surprising since, first, the temperature 0.69 K lies beyond the range of the present investigation. As is known, above about 0.7 K the phonon and roton excitations of the ^{4}He fluid cannot be already negligible,[7,23] and their contribution into the BBP parameter should be considered. In the present study this effect is completely disregarded. Sec-

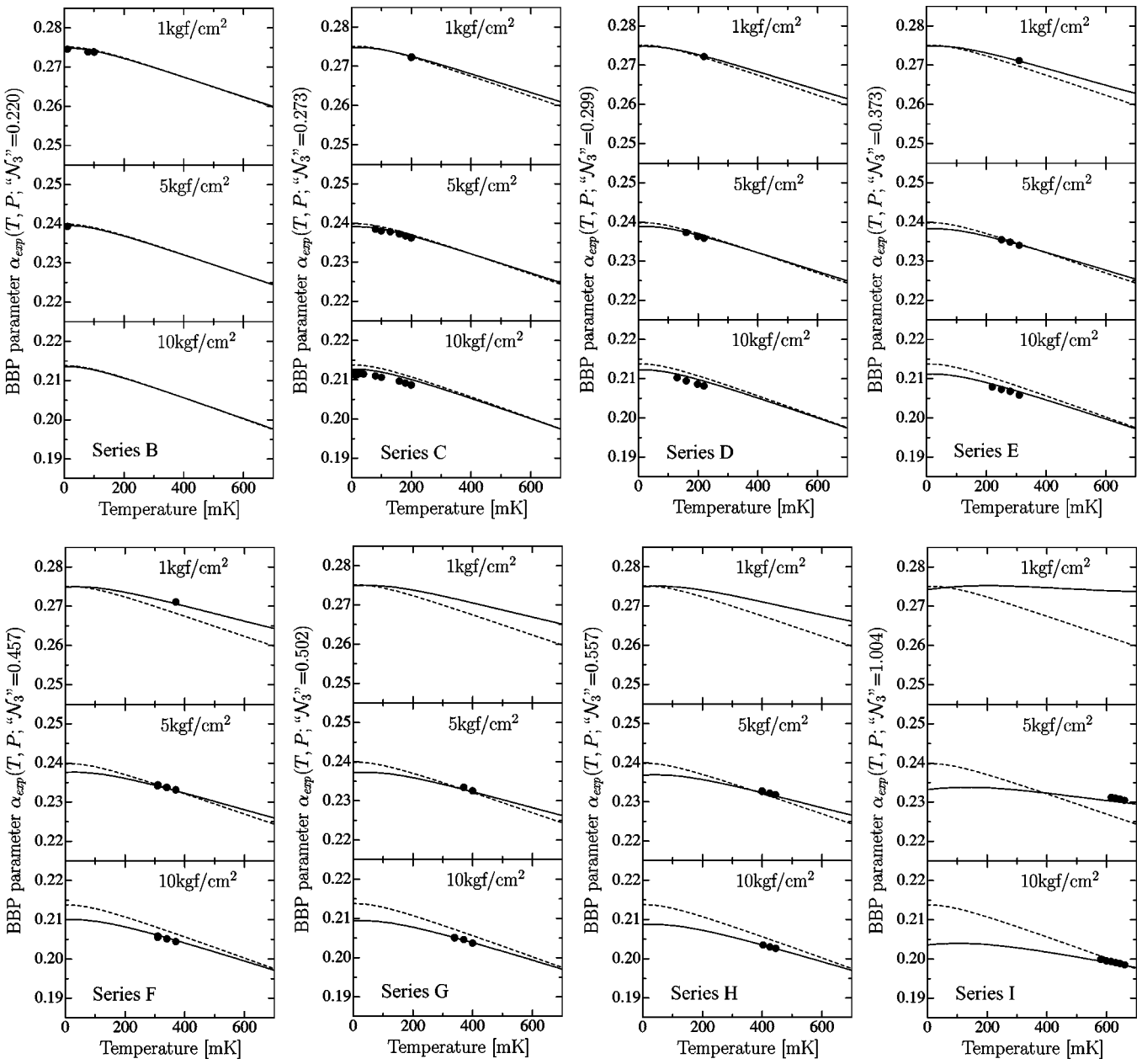

FIG. 14. Experimentally determined BBP parameter $\alpha_{exp}(T,P;\text{“}\mathcal{N}_3\text{”})$ is plotted as a function of temperature at various constant pressures. The solid circles are the data points. The data are for series from B to I as described in Table III. The solid curves are the calculated α_{emp} of Eq. (69). The dashed curves are the calculated $\alpha_{emp,\mathrm{A}}$ of Eq. (68).

ond, the data[4] do not demonstrate any monotonic behavior as a function of concentration within their experimental accuracy. Apparently, this may be attributed to some disadvantages of the measurement procedure resulting in the larger out-of-control errors.

The temperature dependence of the BBP parameter under the saturated vapor pressure is reported in Ref. 5 for an $x=0.055$ solution. In the present study, the comparison between α_{exp} and α_{emp} is made for the temperature dependence at various constant pressures as shown in Figs. 9 and 14, in order to separate definitely the concentration dependence. So, it may be interesting to compare the data of (Ref. 5) with our α_{emp}. The results are shown in Fig. 17(a). It is seen that the agreement is better than 1% though there is a systematic difference between our α_{emp} and the data[5]. Comparing Figs. 17(a) and (b), we recognize that the temperature dependence is mainly due to that of α_{20}.

In order to see the general feature of the approximation with respect to x in Eq. (69), we examine the limit $x=1$. The value of the BBP parameter at $x=1$ may be formally defined as

$$\alpha(T,P,x=1)=\frac{V_{30}(T,P)}{V_{40}(T,P)}-1, \tag{73}$$

which is calculated with $V_{40}(T,P)$[12] and $V_{30}(T,P)$.[22] From Eqs. (68), (69), and (73), we obtain, for example,

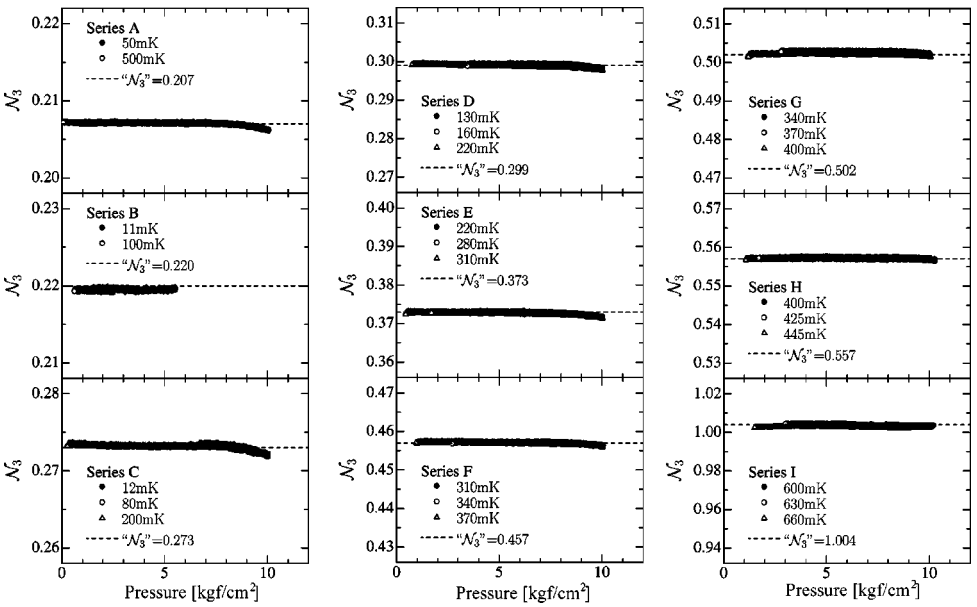

FIG. 15. The values of $\mathcal{N}_3$ obtained from Eq. (72). The data are for series from A to I as described in Table III.

$$\alpha_{emp}(0,0,x=1)=0.3034$$
$$<\alpha(0,0,x=1)=0.3370$$
$$<\alpha_{emp,\mathrm{A}}(0,0,x=1)=0.3618. \quad (74)$$

This result seems reasonable, because we should take into account the terms of higher order with respect to x as x increases, and we may expect the sign of the successive terms to change alternately.

D. Argument on the absolute uncertainty

In the procedure to fix the functional form of α_{emp}, we use the exact formula for α_{20} which mainly contributes to the temperature dependence of the BBP parameter. The main pressure dependence of the BBP parameter comes from α_1. This is determined consistently with $\tilde{\alpha}_3$, which is a functional of α_1 and depends on the ^{3}He concentration. Note that all the fittings agree well with the plot of the data for the temperature dependence of the BBP parameter at various constant pressures (Figs. 9 and 14). It is almost impossible to separate the concentration dependence of $\tilde{\alpha}_3$ from the raw plot of the data shown as the pressure dependence [Figs. 5(b) and 13], since the variation of the BBP parameter with pressure is so large that the concentration dependence is nearly smeared out. Thus, we may say that in the formula of α_{emp} the dependence on temperature, pressure, and the ^{3}He con-

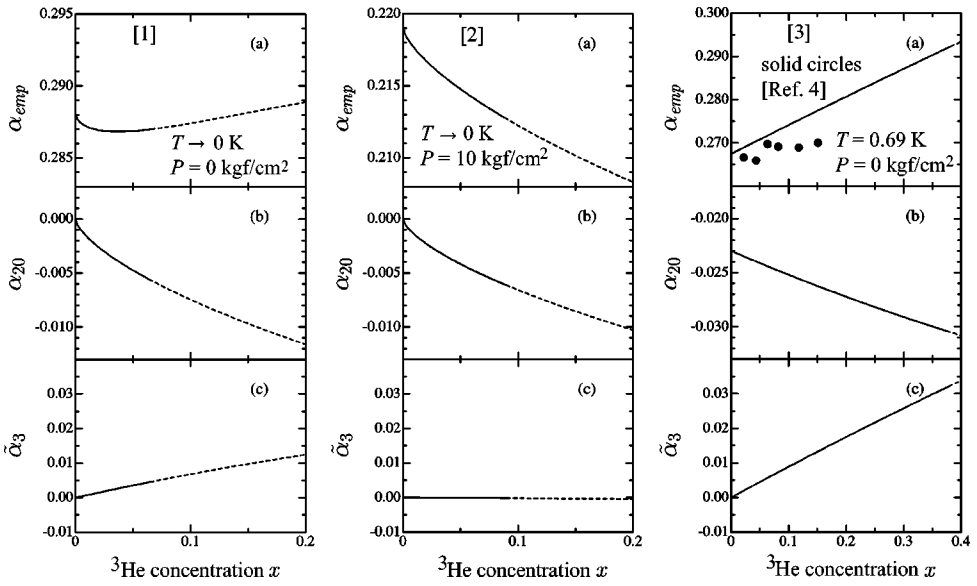

FIG. 16. Concentration dependence of the BBP parameter at various constant temperatures and pressures. (a) The ^{3}He concentration dependence of the BBP parameter calculated from $\alpha_{emp}(T,P,x)$ of Eq. (69). (b) The ^{3}He concentration dependence of α_{20} of Eq. (47). (c) The ^{3}He concentration dependence of $\tilde{\alpha}_3$ in Eq. (69), i.e., $\tilde{\alpha}_3=A_{31}(T,P)x+A_{32}(T,P)x^2$. In each curve, the dashed part corresponds to the region above the saturated concentration.

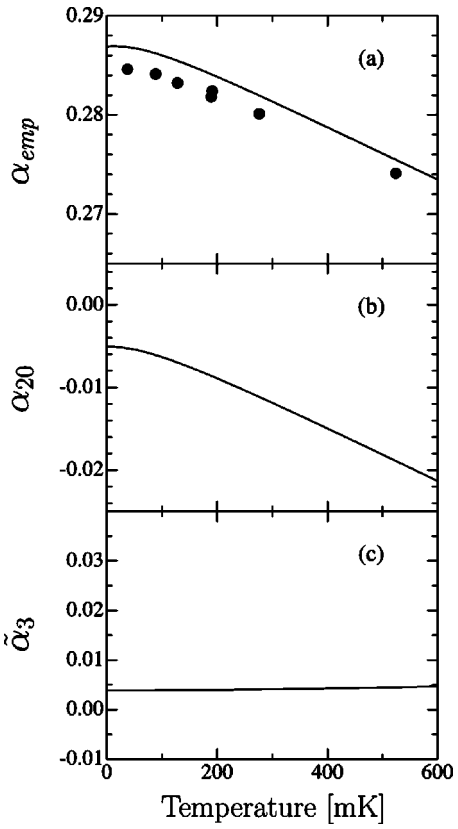

FIG. 17. Temperature dependence of the BBP parameter for the solution of $x=0.055$ at $P=0$. (a) The calculated $\alpha_{emp}(T,0,0.055)$ [the solid curve] and the data from Ref. 5 [the solid circles]. (b) The calculated $\alpha_{20}(T,0,0.055)$. (c) The calculated $\tilde{\alpha}_3(T,0,0.055)$.

centration is correctly grasped. The results of comparison with the completely independent data of other groups as shown in Figs. 16[3] and 17 may support this statement.

In this section we give an argument on the absolute uncertainty of the value obtained with α_{emp}, i.e., that of α_{exp} with which α_{emp} is determined.

Besides the fundamental quantity of Eq. (4) and the related assumptions (for details, see Ref. 12), our values of α_{exp} rely on Refs. 6 and 13 through Eqs. (10) and (13). So, the absolute uncertainty of α_{exp} is closely related to that in the fittings of Eqs. (10) and (13), especially, Eq. (10). For the molar volume of pure liquid ^{4}He $V_{40}(T,P)$, the difference between the present study and Ref. 6 is within $\pm 1 \times 10^{-2}$ cm^3/mol.[12] So, there seems no serious difference in the relative accuracy for the measurement of molar volume between the present study and Ref. 6.

Note that Ref. 6, in turn, relies on Ref. 4 through the empirical formula of α originally given for very dilute mixtures,[4]

$$\alpha(T,0,x\rightarrow 0)=(0.284\pm 0.005)-[(0.032\pm 0.003)\ \ \mathrm{K}^{-1}]T. \tag{75}$$

Watson *et al.* utilized Eq. (75) for a double purpose, in which the applicability of Eq. (75) is extended to the mixture of a rather high concentration and the concentration-, temperature-, and pressure-independent behavior of the coefficient 0.032 K^{-1} is assumed as well. First, they fixed the value of their BBP parameter α_{W} in a single phase region at their normalization point ($T=T^*$, $P=0$) for each run with $x=0.0827$, 0.0918, and 0.100 solutions by

$$\alpha_{\mathrm{W}}(T^*,0;x)\equiv 0.284-0.032T^*. \tag{76}$$

With this normalization, $\alpha_{\mathrm{W}}(T^*,P;x)$ is determined by measuring the pressure dependence of the molar volume at T^*. The temperature T^* is around 0.3 K. Next, Eq. (75) is employed again to estimate $\alpha_{\mathrm{W}}(0.05,P;x)$ as

$$\alpha_{\mathrm{W}}(0.05,P;x)=\alpha_{\mathrm{W}}(T^*,P;x)+0.032(T^*-0.05). \tag{77}$$

With $\alpha_{\mathrm{W}}(0.05,P;x)$ thus estimated, the saturated concentration $x_{s,\mathrm{W}}(0.05,P)$ is determined by using Eq. (2) from the measurements of the molar volume for the d-phase as a function of pressure in the phase-separated state.

Note that the pressure dependence of the saturated concentration $x_s(T,P)$ is mainly related with the pressure dependence of the BBP parameter. The effect of the concentration variation due to the pressure on the BBP parameter is almost negligible for determining the pressure dependence of the saturated concentration.

As can be seen from Figs. 9, 14, and 17, the temperature dependence of α_{emp} is not a simple T-linear behavior as is assumed in Eq. (77). However, as is seen in Figs. 9 and 14, the temperature behavior of α_{emp} does not show any appreciable pressure dependence for a fixed "$\mathcal{N}_3$." From Fig. 14, it is seen that the temperature dependence varies with the amount of "$\mathcal{N}_3$." That is, the temperature dependence is expected to vary with the ^{3}He concentration. However, it may be plausible to neglect this effect for α_{W} since the variation of the concentration within $x=0.0827$–0.100 is not so large. So, one may expect that $\alpha_{\mathrm{W}}(0.05,P;x)$ estimated with Eq. (77) represents the sufficiently correct behavior of the relative pressure dependence. Taking into account the statement in the beginning of this section, we may say that the absolute uncertainty of our $\alpha_{emp}(T,P,x)$ is that of $\alpha_{\mathrm{W}}(0.05,P;x)$ or $x_{s,\mathrm{W}}(0.05,P)$ almost regardless of temperature and the ^{3}He concentration.

In Fig. 8 of Ref. 6, one recognizes that the $x=0.0827$ solution remixes at about 3 atm pressure. The concentration at this remixing region is given as about 0.0820 with α_{W}. So, the uncertainty of $\alpha_{\mathrm{W}}(0.05,P)$ seems to be 1–1.5% corresponding to the absolute uncertainty of about 0.001 in ^{3}He concentration. For the averaged values of $x_{s,\mathrm{W}}(0.05,P)$ given in Table III of Ref. 6 and used in our Eq. (10), the absolute uncertainty is also stated as ± 0.001. This means that the absolute uncertainty, expressed in fractions of $x_{s,\mathrm{W}}(0.05,P)$, does not exceed 1.5% for $P=0$ and 1% for $P=10$ kgf/cm^2 according to the increase of the saturated concentration with pressure within this range. Consequently, we may conclude that, on the whole, the absolute uncertainty of our α_{emp} lies within 1–1.5% depending slightly on pressure and almost irrespective of temperature and the ^{3}He concentration.

V. SUMMARY

We have presented the experimental data of the BBP parameter determined with our new method. The investigated region of temperature is 0.4–660 mK, that of pressure is 0.3–10 kgf/cm^2, and that of the ^{3}He concentration is 0.07–0.39.

In the usual method of obtaining the BBP parameter, one condenses a gas mixture, the ^{3}He concentration of which is known beforehand. The pressure is applied by using the same gas mixture. In the present method, we confine a liquid mixture by a cell and the amount of ^{3}He is kept constant during a series of experiments in which the pressure is swept at various constant temperatures. The pressure is changed by controlling the amount of ^{4}He in the cell. So, the ^{3}He concentration varies mainly as a function of pressure. This is an advantageous aspect of the present method. That is, one can deal with a wide range of the ^{3}He concentration without preparing gas mixtures of various ^{3}He concentrations. The estimation of the amount of the ^{3}He confined in the cell is essential to the present method. This is done consistently with respect to the determination of the BBP parameter.

The second advantageous aspect of our method is associated with lacking the necessity of warming the whole system up in order to prepare in the cell the sample mixture of different concentrations. That is, the calibration procedure of various gauges, e.g., concentration and pressure ones or thermometers, is required only once in the beginning of all experimental runs.

The data obtained are fitted with an appropriate formula based on the phenomenological theory of ^{3}He-^{4}He liquid mixtures. Our empirical formula of Eq. (69) is shown to reproduce the experimental values of the BBP parameter within the accuracy of 1% in the whole ranges of temperature, pressure, and the ^{3}He concentration presently studied. The absolute uncertainty of $\alpha_{emp}(T,P,x)$ is estimated as within 1–1.5% depending slightly on pressure and almost regardless of temperature and the ^{3}He concentration. This is due to our procedure referring to the saturated concentration $x_{s,W}(0.05,P)$ which has the absolute uncertainty ± 0.001 in the ^{3}He concentration. We believe our empirical formula will be useful for various studies of ^{3}He-^{4}He mixtures.

ACKNOWLEDGMENTS

The present work has been performed under Grant-in-Aid for Scientific Research on Priority Area (No. 271) from the Ministry of Education, Science and Culture of Japan (Contract No. 08240203). One of the authors (S.B.) is grateful to the Japan Society for the Promotion of Science and also the Yamada Foundation.

*Corresponding author. Electronic address:
t-satoh@mail.cc.tohoku.ac.jp

[1] J. Bardeen, G. Baym, and D. Pines, Phys. Rev. **156**, 207 (1967).
[2] T. Satoh, M. Morishita, M. Ogata, and S. Katoh, Phys. Rev. Lett. **69**, 335 (1992); T. Satoh, M. Morishita, S. Katoh, K. Hatakeyama, and M. Takashima, Physica B **197**, 397 (1994); E. Tanaka, K. Hatakeyama, S. Noma, S. N. Burmistrov, and T. Satoh, J. Low Temp. Phys. **127**, 81 (2002).
[3] C. Boghosian and H. Meyer, Phys. Lett. A **25**, 352 (1967).
[4] D. O. Edwards, E. M. Ifft, and R. E. Sarwinskii, Phys. Rev. **177**, 380 (1969); E. M. Ifft, D. O. Edwards, R. E. Sarwinskii, and M. M. Skertic, Phys. Rev. Lett. **19**, 831 (1967).
[5] B. M. Abraham, O. G. Brandt, Y. Eckstein, J. Munarin, and G. Baym, Phys. Rev. **188**, 309 (1969).
[6] G. E. Watson, J. D. Reppy, and R. C. Richardson, Phys. Rev. **188**, 384 (1969); G. E. Watson, Ph.D. thesis, Cornell University, 1969.
[7] G. Baym and C. Pethick, *Landau Fermi-Liquid Theory* (Wiley, New York, 1991), p. 137.
[8] E. C. Kerr and R. H. Sherman, J. Low Temp. Phys. **3**, 451 (1970).
[9] T. Tsuda, Y. Mori, and T. Satoh, Rev. Sci. Instrum. **62**, 841 (1991). The present modified version is equipped with the bellows for opening.
[10] G. C. Straty and E. D. Adams, Rev. Sci. Instrum. **40**, 1393 (1969).
[11] C. Boghosian and H. Meyer, Phys. Rev. **152**, 200 (1966).
[12] E. Tanaka, K. Hatakeyama, S. Noma, and T. Satoh, Cryogenics **40**, 365 (2000).
[13] S. Kurikawa, Master's thesis, University of Tokyo, 1988.
[14] K. Huang, *Statistical Mechanics* (Wiley, New York, 1963); W. Greiner, L. Neise, and H. Stöker, *Thermodynamics and Statistical Mechanics* (Springer, New York, 1995).
[15] V. R. Pandharipande and N. Itoh, Phys. Rev. A **8**, 2564 (1973).
[16] R. A. Sherlock and D. O. Edwards, Phys. Rev. A **8**, 2744 (1973); E. Polturak and R. Rosenbaum, J. Low Temp. Phys. **43**, 477 (1981).
[17] C. Ebner, Phys. Rev. **185**, 392 (1969).
[18] A. C. Anderson, D. O. Edwards, R. Roach, R. E. Sarwinskii, and J. C. Wheatley, Phys. Rev. Lett. **17**, 367 (1966); W. R. Abel, R. T. Johnson, J. C. Wheatley, and W. Zimmerman, Jr., *ibid.* **18**, 737 (1967).
[19] P. Seligman, D. O. Edwards, R. E. Sarwinski, and J. T. Tough, Phys. Rev. **181**, 415 (1969).
[20] C. Ebner and D. O. Edwards, Phys. Rep. C **2**, 77 (1971).
[21] J. Landau, J. T. Tough, N. R. Brubaker, and D. O. Edwards, Phys. Rev. A **2**, 2472 (1970).
[22] B. M. Abraham and D. W. Osborne, J. Low Temp. Phys. **5**, 335 (1971).
[23] M. Morishita, T. Kuroda, A. Sawada, and T. Satoh, J. Low Temp. Phys. **76**, 387 (1989).